Supporting Information

Polyoxometalate-Embedded Cu-Triazole Cycle: Catalytic Oxidation of Alcohols

Quanzhong Wang, Yahong Chen, Fengshou Tian and Ruixia Dou*

College of Chemistry and Chemical Engineering, Zhoukou Normal University, Zhoukou, 466001, Henan, P. R.

Section 1. Experiment Section

Materials and methods. All chemicals and reagents were obtained from already available commercially certified reagent sources and were used without any further purifications unless mentioned. $K_6Na_2[GeW_{11}O_{39}]\cdot 13H_2O$ was synthesized accroding to the literature and characterized by IR spectroscopy.[1] The elemental analyses (EA) of C, H and N were performed on a Vario EL III elemental analyzer. The Inductively Coupled Plasma Optical Emission Elemental analyses of Ge and W were performed on a Jarrel-Ash Model J-A1100 spectrometer. IR spectra were recorded in the range of 400−4000 cm^{-1} on a JASCO FT/IR-430 spectrometer with pressed KBr pellets. The thermogravimetric analysis was performed on a Mettler-Toledo TGA/SDTA 851e instrument heated from 25 to 800 °C with a heating rate of 10 °C min^{-1}, under a dynamic nitrogen atmosphere. The powder X-ray powder diffraction (PXRD) patterns were carried out on a Bruker D8. Advance instrument with Cu Kα radiation (λ = 1.5418 Å). X-ray photoelectron spectra (XPS) were recorded

with an Axis Ultra X-ray photoelectron spectrometer. GC analyses were performed on a Bruker 450-GC with a flame ionization detector equipped with a 30 cm column (GsBP-5, 0.25 mm internal diameter and 0.25 μm film thickness) with nitrogen as carrier gas.

Single crystal X–ray Crystallography. Single-crystal X-ray data were carried out on a collected on Bruker D8 VENTURE PHOTON II CCD diffractometer detector at 150 K with Mo Kα radiation (λ = 0.71073 Å). Intensity data were using Olex2, the structure was solved with the Olex2. Solve structure solution program using Charge Flipping and refined with the Olex2 refinement package using Gauss-Newton minimisation.[2,3] All H atoms on water molecules were directly included in the molecular formula. A summary of crystal data and structure refinements for compound **Cu-W-TRZ** is provided in Table S6.

The Procedure of the Catalysis. The catalytic studies were performed on various alcohols using **Cu-W-TRZ**. The alcohols (1 mmol), tert-butyl hydroperoxide (TBHP) (3 mmol) catalyst (0.2 mol%), and CH_3CN (1 mL) were added into a tube at room temperature. The mixture was further stirred under the prescribed conditions on the parallel reactor. All of target products were identified by GC−MS, and the yields were monitored by GC with methylbenzene as internal standard. The catalyst was recovered by filtration when the reaction mixture was cooled to room temperature at the end of each

cycle, and then washed thoroughly (at least three times) with acetonitrile, and dried in an oven at 90 °C overnight to be reused for the next round.

XPS Test. The peaks at 933.16 eV and 952.87 eV corresponded to the binding energy of $Cu2p^{3/2}$ and $Cu2p^{1/2}$, which originated from Cu^{+} (CuCl and Cu_2O). The peaks at 935.44 eV, 944.53 eV and 955.26 eV corresponded to the binding energy of $Cu2p^{3/2}$ and $Cu2p^{1/2}$, which originated from Cu^{2+} ($CuCl_2$ and CuO or $Cu(OH)_2$). And the Cu^{+} constituted the main part. After oxidation reaction, Cu^{+} ions in **Cu-W-TRZ** are not oxidized, which also proves the stability of the catalyst to some extent.[4]

U_{TBHP} was calculated by the equation:

$$U_{TBHP} = \frac{moles moles\ of\ products\ being\ formed}{moles\ of\ TBHP\ \mathrm{int}\ itial - moles\ of\ TBHP\ finial} \times 100\% \quad \text{(Eq.S1)}$$

The amount of TBHP was determined by titrated with 0.1 M $Na_2S_2O_3$ solution.

Section 2 Schemes Section

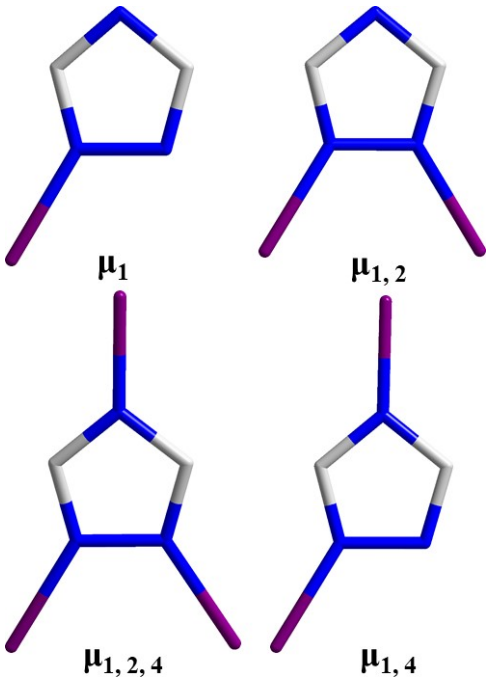

Scheme S1. Four Coordination Modes of 1,2,4-Triazole Ligands.

Section 3 Figures Section

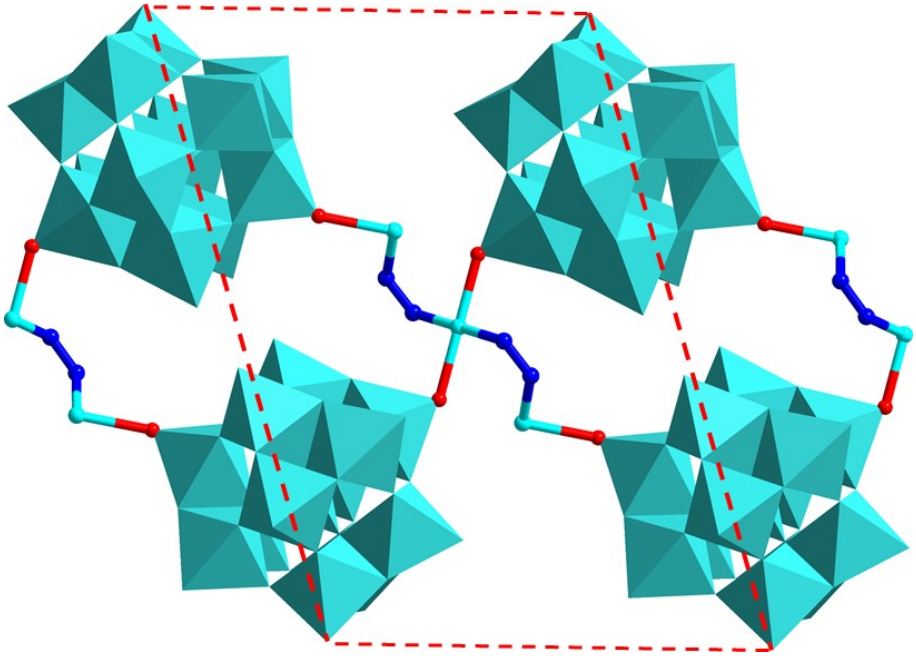

Figure S1. The structure of four adjacent {GeW_{12}} polyanions.

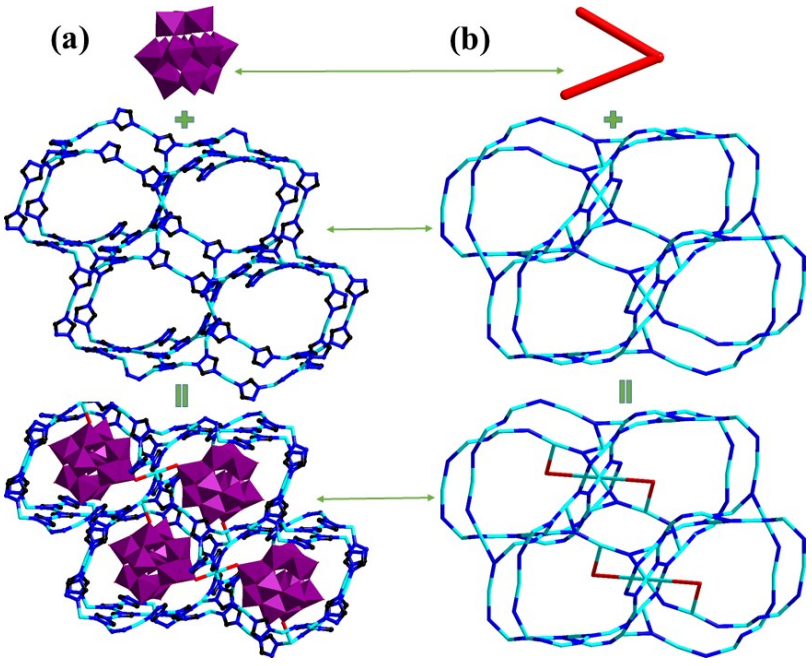

Figure S2. (a) The 3D framework of and (b) the 3D topology network of **Cu-W-TRZ**.

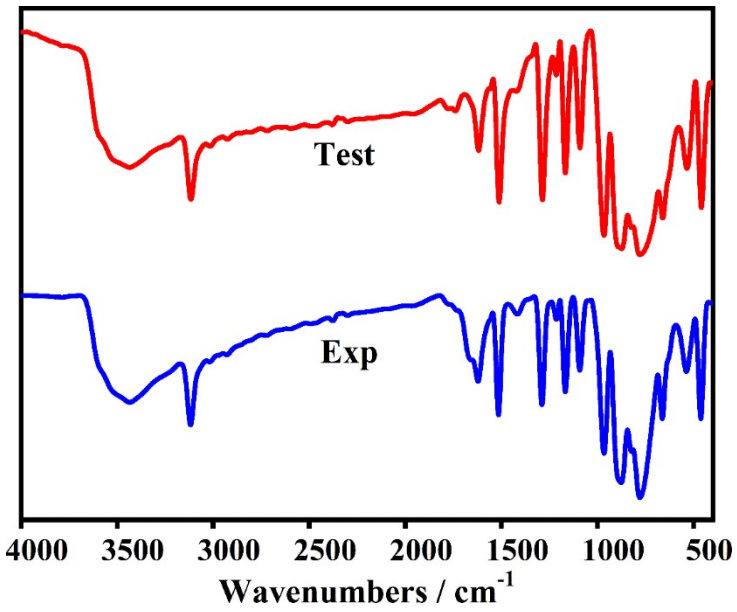

Figure S3. The IR spectrum of **Cu-W-TRZ** fresh and test between 4000 and 400 cm^{-1}.

The infrared spectrum of **Cu-W-TRZ** clearly shows, the characteristic peaks at 1091, 968, 881 and 797 cm^{-1}, which all vest in νas (W–Ot), νas (W–Ob–W), νas (P–Oa), and νas (W–Oc–W) of the $\{GeW_{12}\}$ polyanion (Figure S3), respectively. Additionally, the presence of vibrational bands at 1300 cm^{-1} is in agreement with the presence of the C=N vibrations of TRZ.

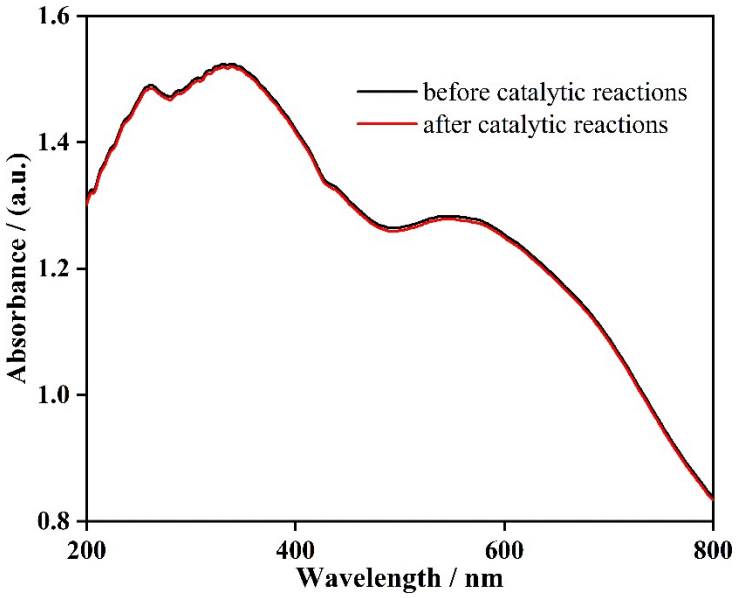

Figure S4. UV-Vis spectra of **CuW-TRZ** before (black) and after (red) during the catalytic oxidation of alcohols.

$$-\frac{dC_t}{d_t} = kC_t \quad (1)$$

$$\ln\frac{C_0}{C_t} = kt \quad (2)$$

$$\ln k = -E_a / RT + \ln A \quad (3)$$

$$\Delta H^{\neq} = E_a - RT \quad (4)$$

$$K = \frac{K_B T}{h}(c^{\Theta})\exp(\frac{\Delta_r^{\neq} S_m^{\Theta}(c^{\Theta})}{R})\exp(\frac{\Delta_r^{\neq} H_m^{\Theta}(c^{\Theta})}{RT}) \quad (5)$$

$$\Delta G^{\neq} = \Delta H^{\neq} - T\Delta S^{\neq} \quad (6)$$

Figure S5. Related equations on Mechanism Research.

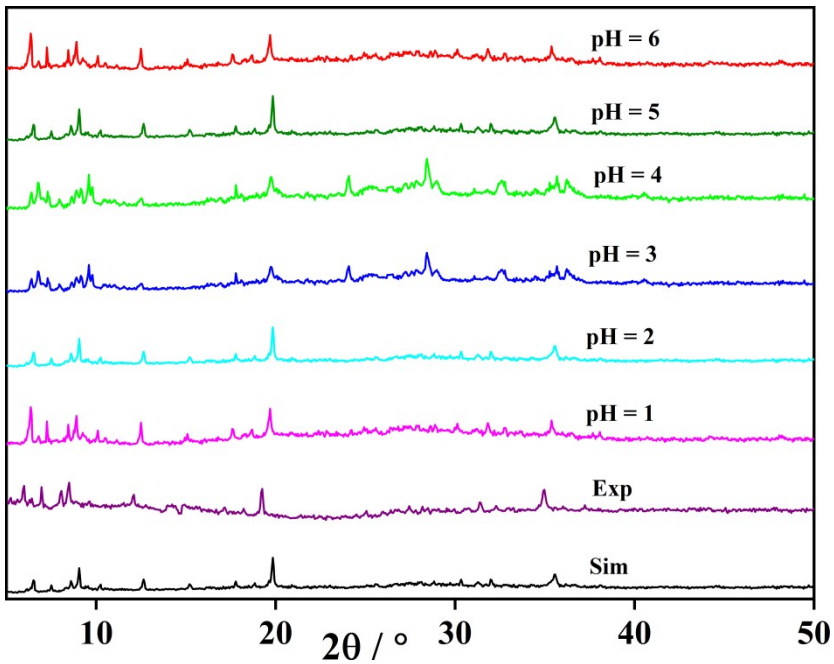

Figure S6. PXRD patterns of **CuW-TRZ** after 24 h immersion in acidic aqueous solutions with the pH range of 1-6.

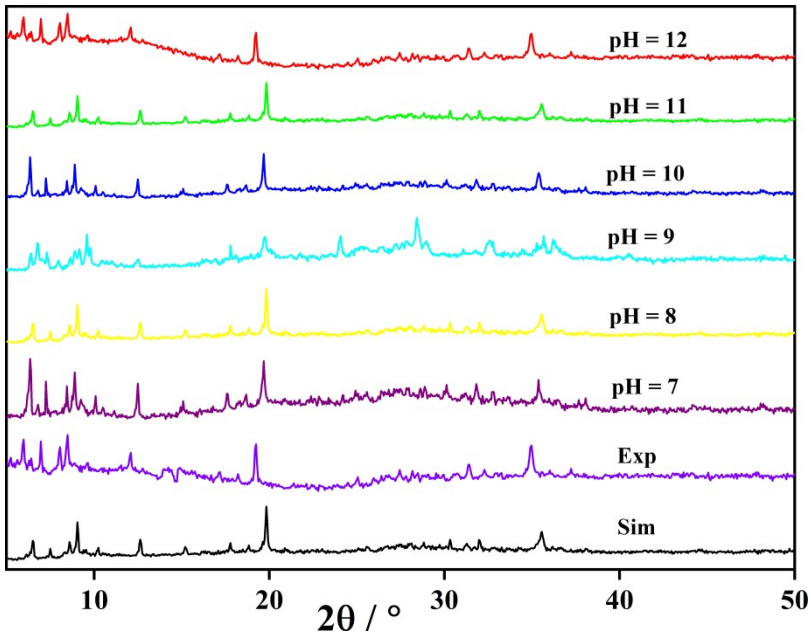

Figure S7. PXRD patterns of **CuW-TRZ** after 24 h immersion in basic aqueous solutions with the pH range of 7-12.

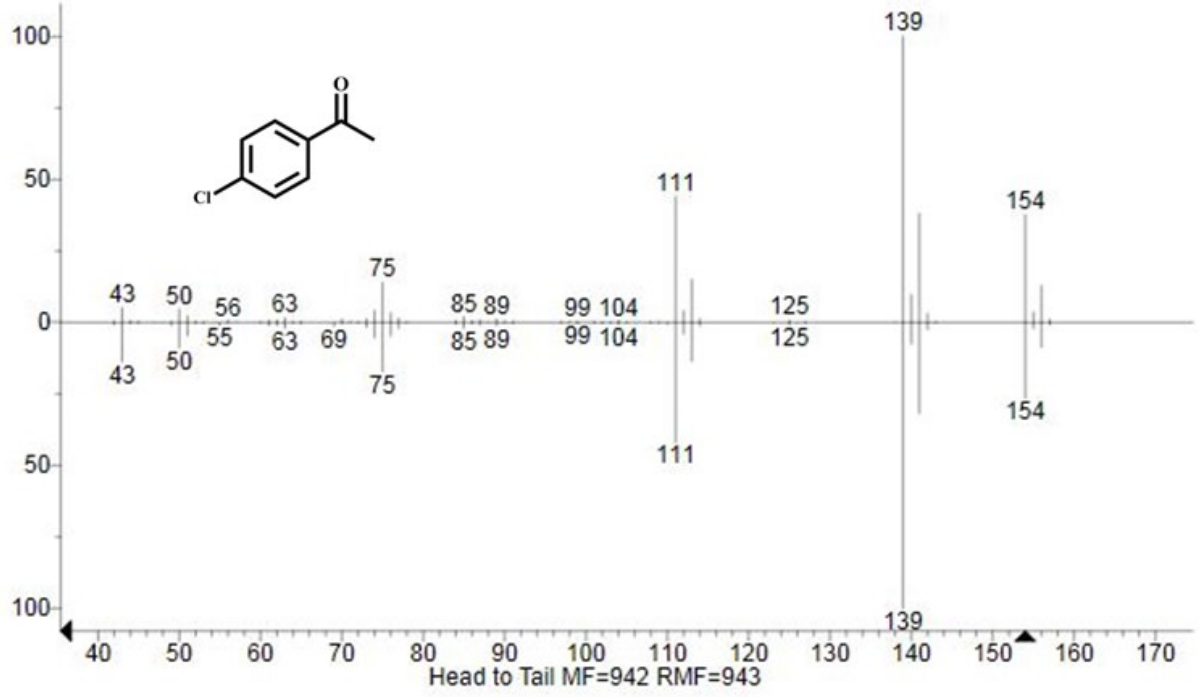

Figure S8. GC-Mass spectrum of 4-chloro-1-phenylethyl ketone (Top: experimental value; bottom: standard value).

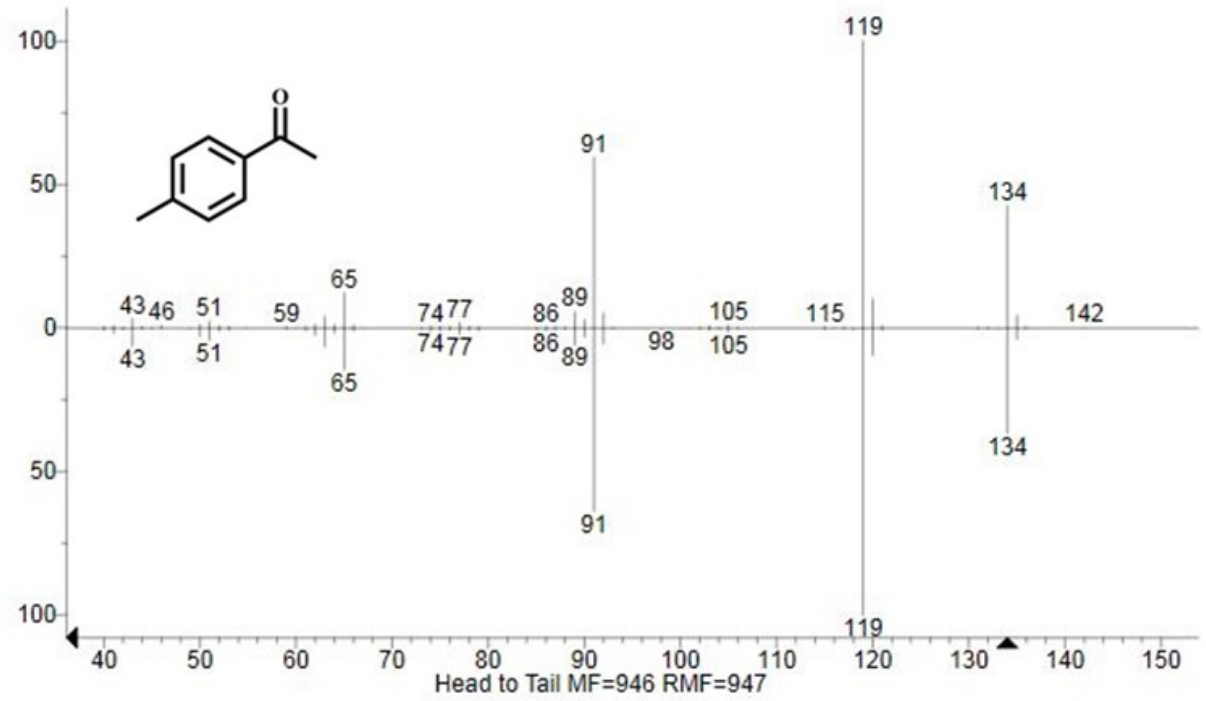

Figure S9. GC-Mass spectrum of 4-methyl-1-phenylethyl ketone (Top: experimental value; bottom: standard value).

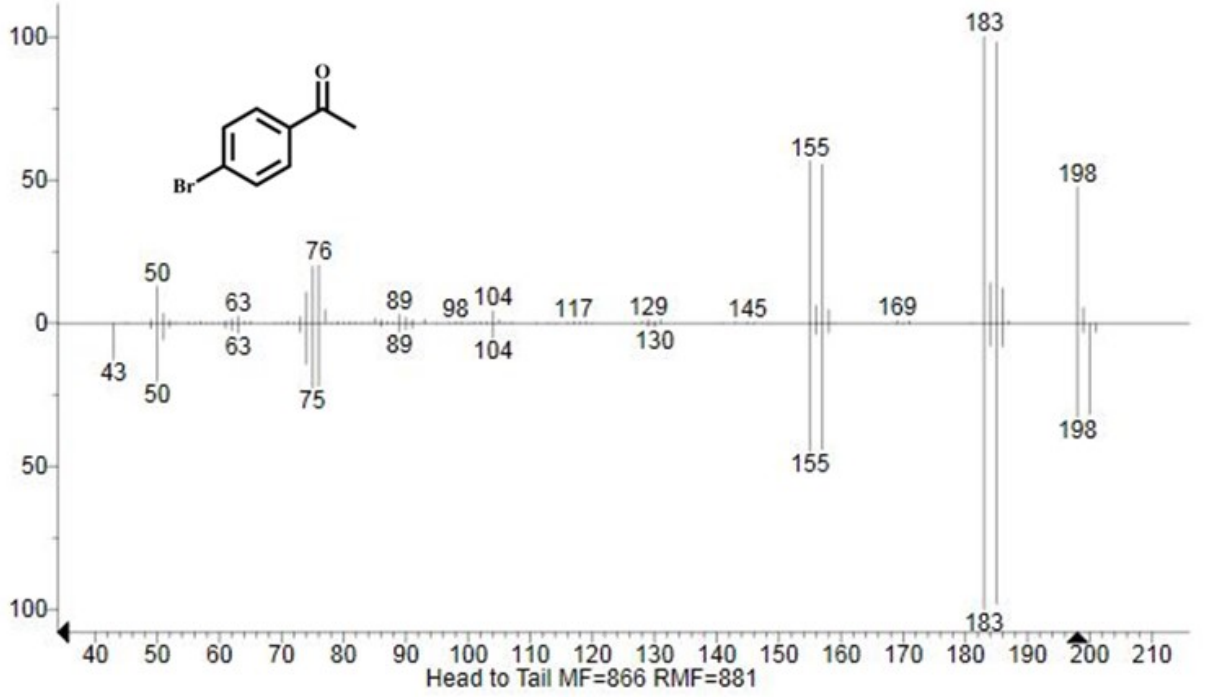

Figure S10. GC-Mass spectrum of 4-bromine -1-phenylethyl ketone (Top: experimental value; bottom: standard value).

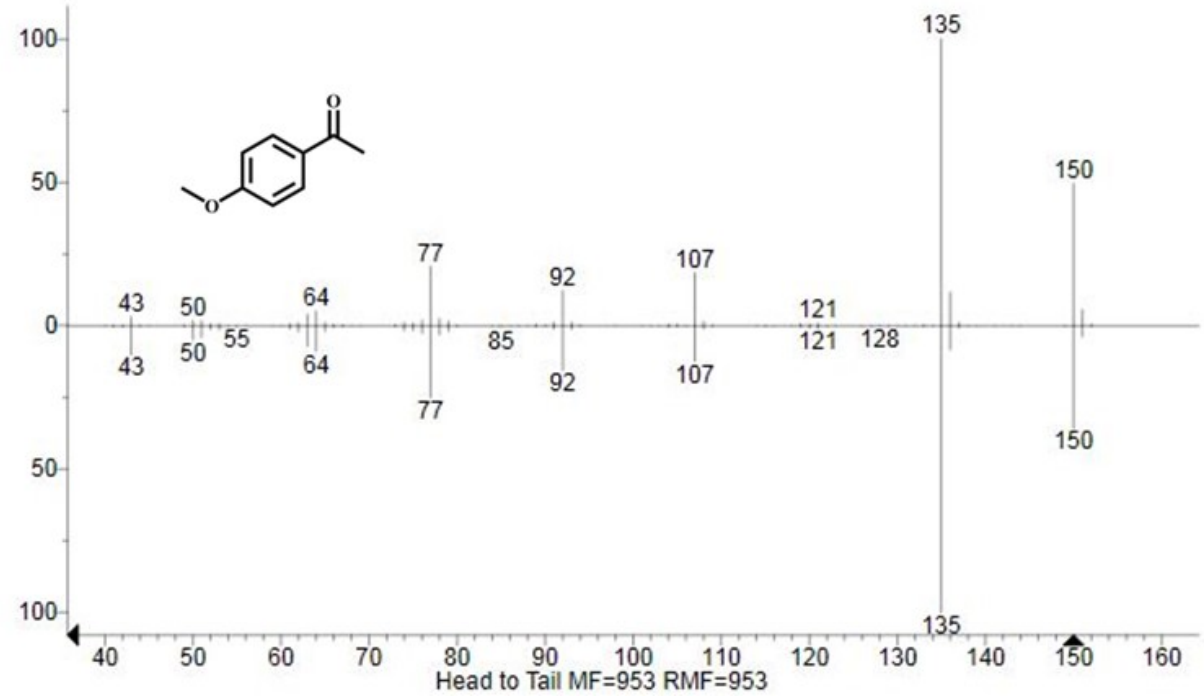

Figure S11. GC-Mass spectrum of 4-methoxy -1-phenylethyl ketone (Top: experimental value; bottom: standard value).

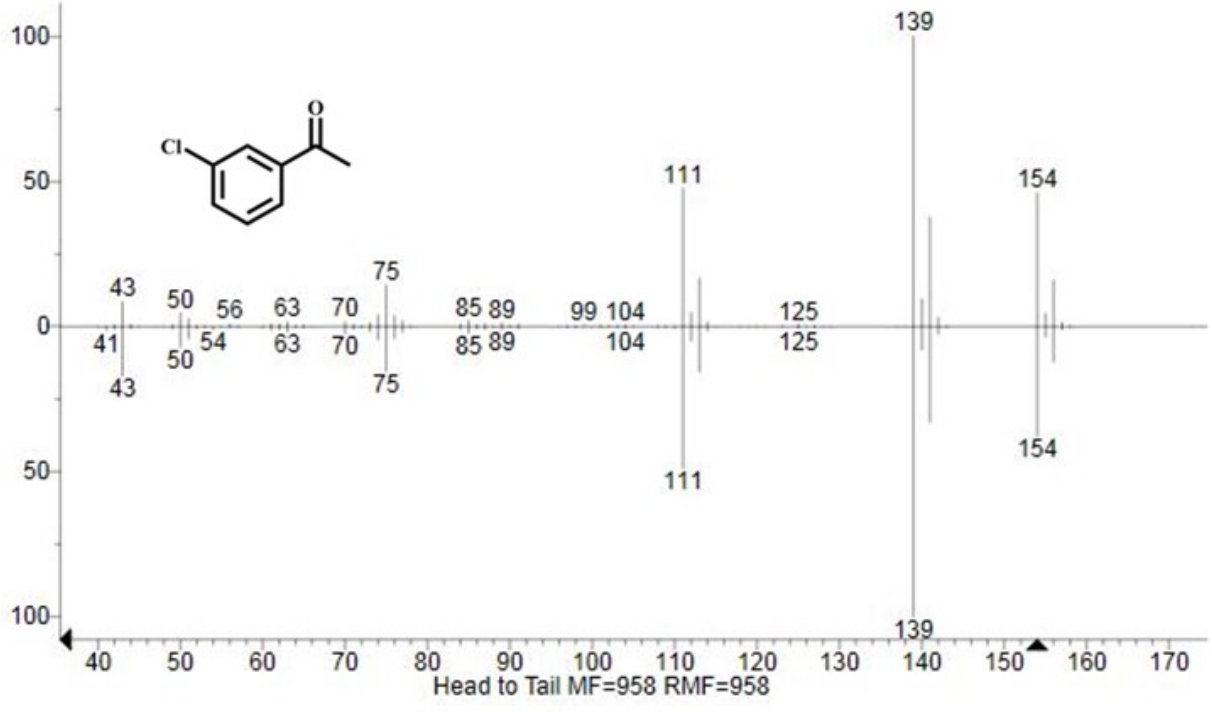

Figure S12. GC-Mass spectrum of 3-chloro-1-phenylethyl ketone (Top: experimental value; bottom: standard value).

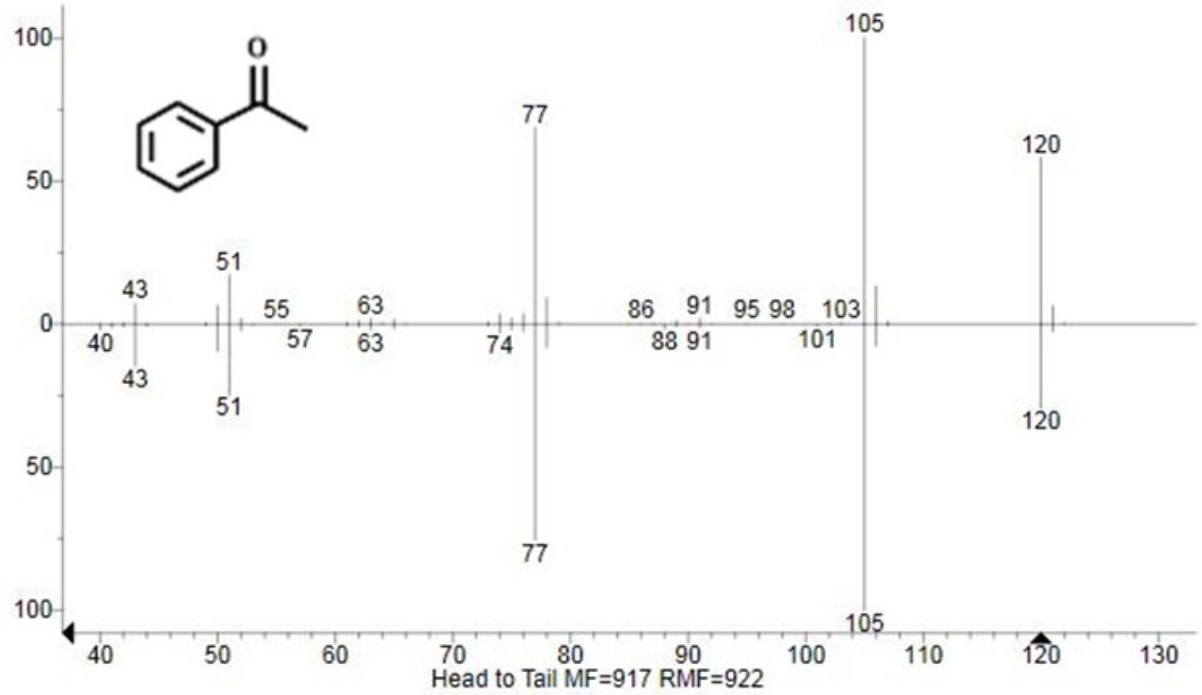

Figure S13. GC-Mass spectrum of phenylethyl ketone (Top: experimental value; bottom: standard value).

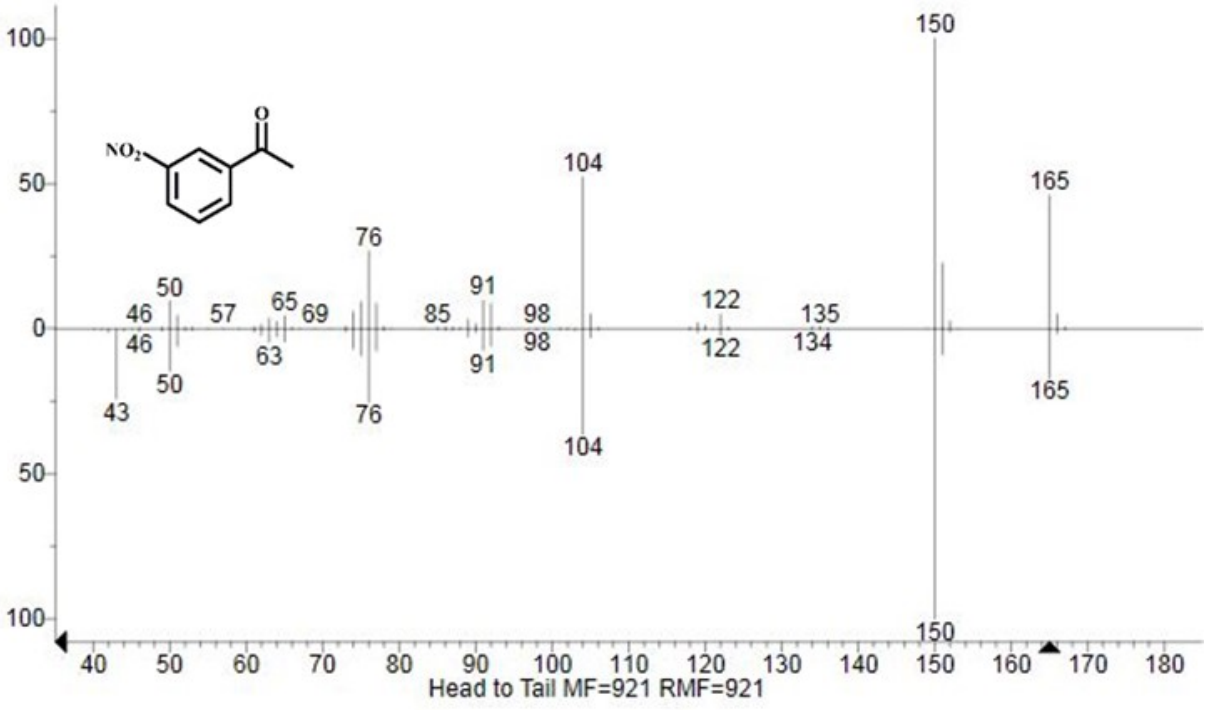

Figure S14. GC-Mass spectrum of 3-nitro-1-phenylethyl ketone (Top: experimental value; bottom: standard value).

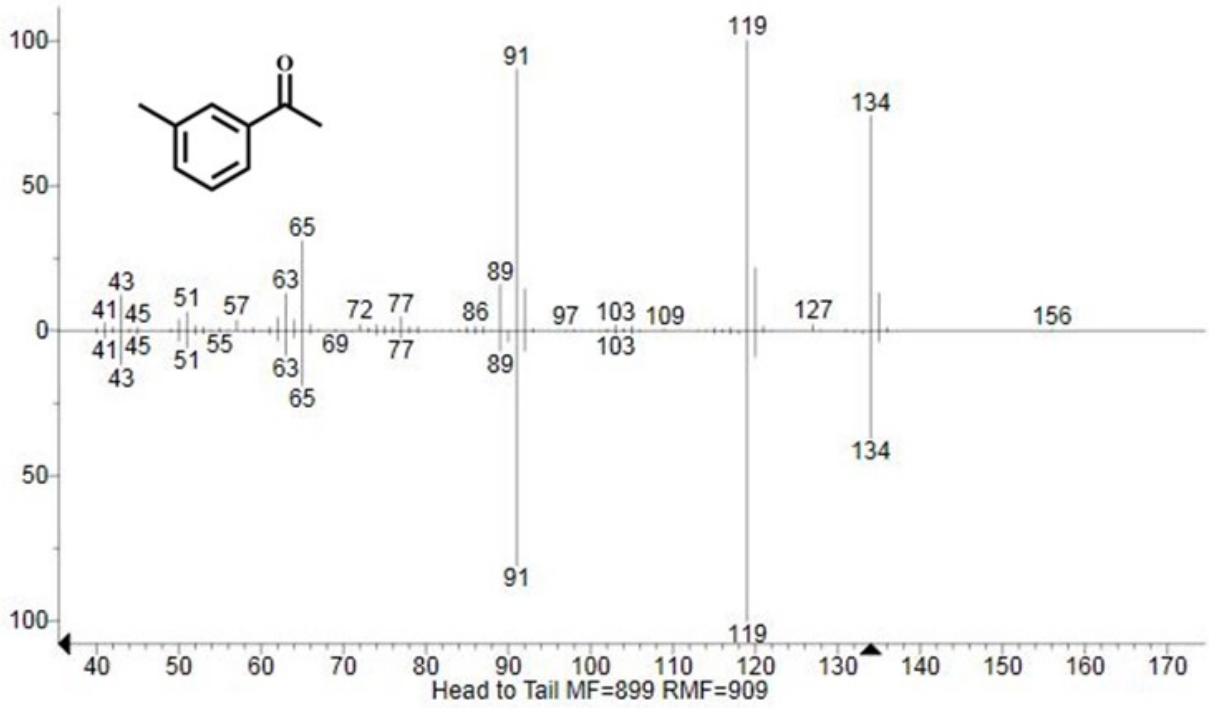

Figure S15. GC-Mass spectrum of 3- methyl -1-phenylethyl ketone (Top: experimental value; bottom: standard value).

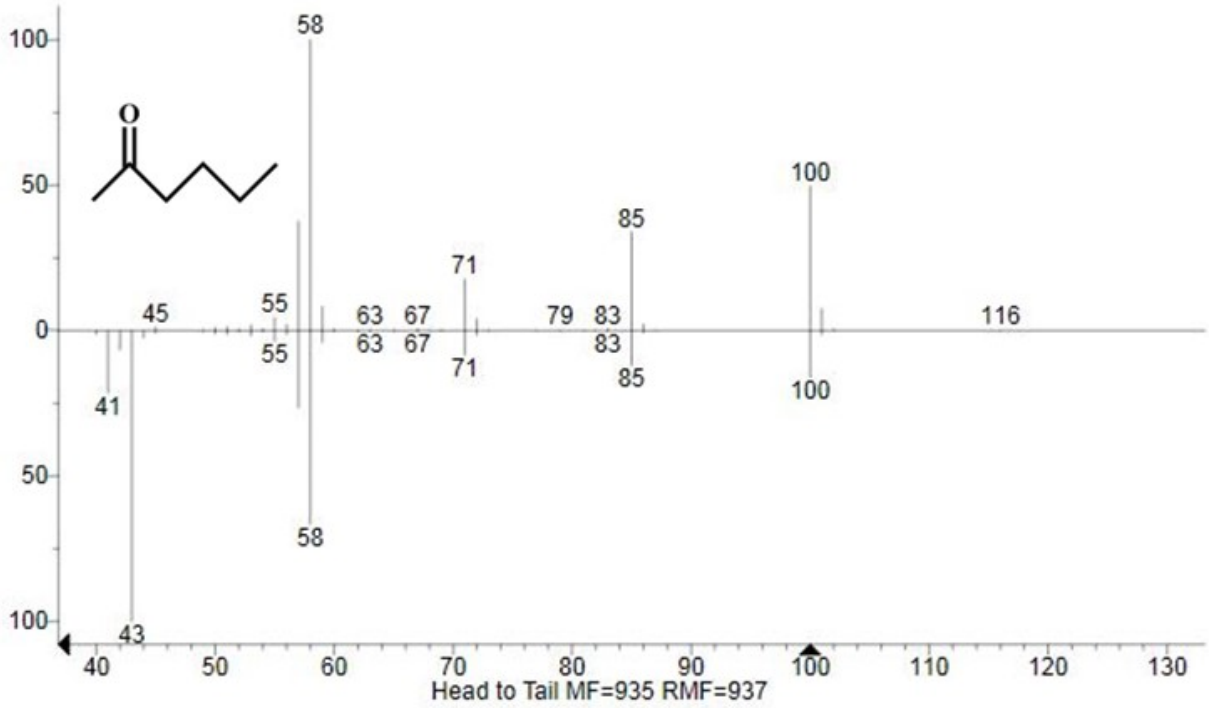

Figure S16. GC-Mass spectrum of 2-hexanone (Top: experimental value; bottom: standard value).

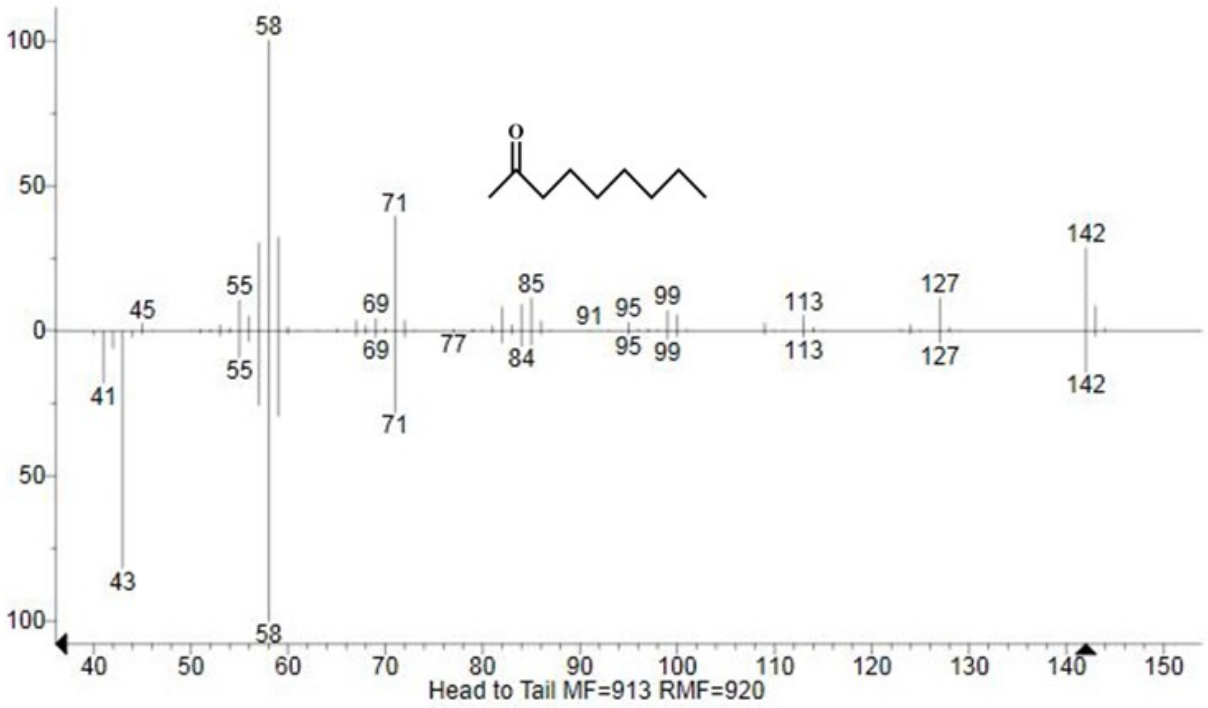

Figure S17. GC-Mass spectrum of 2-nonyl ketone (Top: experimental value; bottom: standard value).

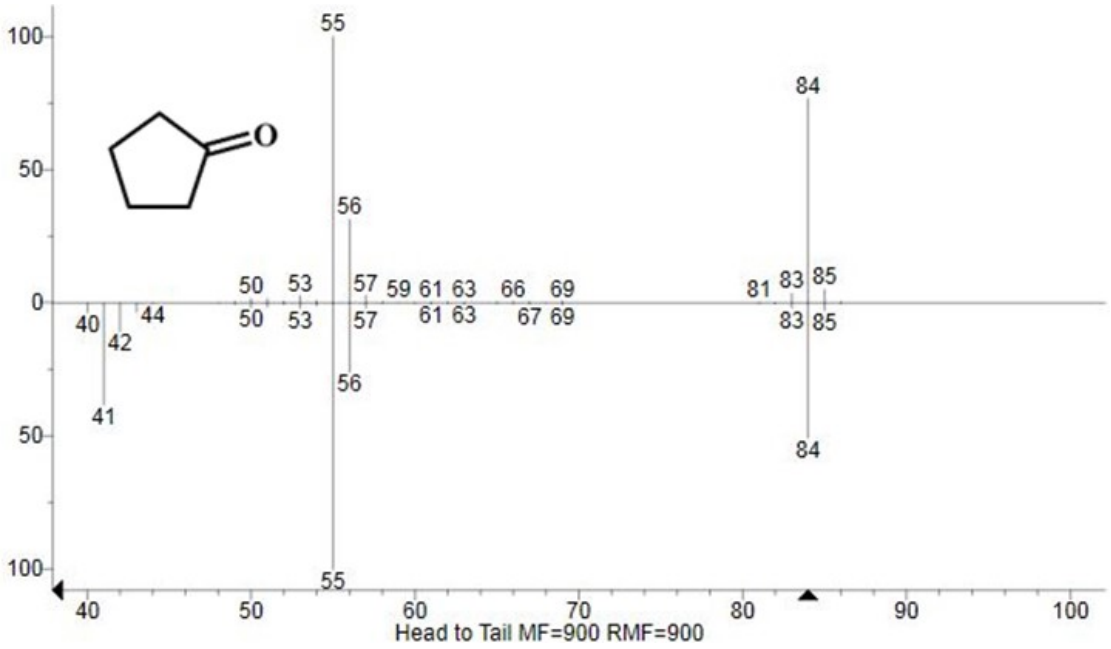

Figure S18. GC-Mass spectrum of cyclohexanone (Top: experimental value; bottom: standard value).

Section 4 Tables Section

Table S1. Selected bond lengths (Å) of **CuW-TRZ**

Bond	Bond Length	Bond	Bond Length
Cu1—N2	1.990(9)	Cu6—N12^{2}	2.003(9)
Cu1—N4^{1}	2.013(9)	Cu6—N14	1.968(9)
Cu1—N2^{1}	1.990(9)	Cu5—O41	1.907(7)
Cu1—N4	2.013(9)	Cu6—N16	2.020(10)
Cu1—O10^{1}	2.343(6)	Cu6—N19	1.970(9)
Cu1—O10	2.343(6)	Cu7—N8	1.865(8)
Cu2—N6	1.865(9)	Cu7—N15	1.877(9)
Cu2—N7	1.857(9)	Cu8—N11^{2}	1.991(8)
Cu3—N3	1.996(8)	Cu8—N11^{5}	1.991(8)
Cu3—N5	1.975(8)	Cu8—N17	2.003(9)
Cu3—N10^{2}	2.000(8)	Cu8—N17^{6}	2.003(9)
Cu3—O1^{3}	2.429(9)	Cu5—N9^{2}	1.989(8)
Cu4—N21^{4}	1.911(10)	Cu5—N13	1.996(8)
Cu4—N1	1.907(10)	Cu5—N20	2.019(8)

Table S2. Selected bond angles (º) of **CuW-TRZ**

Bond	Bond Angle	Bond	Bond Angle
N2^{1}—Cu1—N2	180.0(4)	N1—Cu4—N21^{4}	170.8(4)
N2^{1}—Cu1—N4^{1}	91.7(4)	N9^{2}—Cu5—N13	174.6(4)
N5—Cu3—N10^{2}	169.2(4)	N13—Cu5—N20	93.6(3)
N2—Cu1—N4^{1}	88.3(4)	N9^{2}—Cu5—N20	90.3(3)
N2^{1}—Cu1—N4	88.3(4)	N5—Cu3—N3	90.1(3)
N2—Cu1—N4	91.7(4)	N12^{2}—Cu6—N16	90.3(4)
Cu3—O41—Cu5	123.6(4)	N8—Cu7—N15	178.9(4)
N11^{6}—Cu8—N17	91.6(4)	N14—Cu6—N12^{2}	177.1(3)
N11^{6}—Cu8—N17	88.4(4)	N14—Cu6—N16	91.6(4)
N11^{2}—Cu8—N17^{5}	91.6(4)	N14—Cu6—N19	90.9(10)
N4^{1}—Cu1—N4	180.0	N11^{2}—Cu8—N11^{6}	180.0
N17^{5}—Cu8—N17	180.0(3)	N11^{2}—Cu8—N17	88.4(4)
N7—Cu2—N6	179.0(4)	N19—Cu6—N12^{2}	86.9(4)
N3—Cu3—N10^{2}	94.5(3)	N19—Cu6—N16	172.0(4)

Table S3. The BVS values in **CuW-TRZ**

atoms	Coordination number	BVS value	Oxidation state
Cu1	6	2.122	+2
Cu2	2	1.326	+1
Cu3	5	2.024	+2
Cu4	2	1.165	+1
Cu5	4	1.860	+2
Cu6	5	2.101	+2
Cu7	2	1.291	+1
Cu8	6	2.013	+2
Ge1	4	4.281	+4
W1-W12	6	5.959-6.255	+6

Table S4. Catalytic oxidation of CPE with different solvents [a].

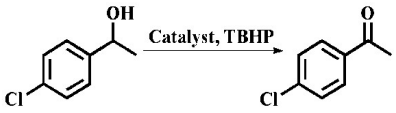

Entry	Solvent	Conv. [b] / %	Sel. / %
1	acetonitrile	99.9	100
2	tetrachloromethane	88.6	91
3	benzonitrile	91.5	100
4	chlorobenzol	80.7	79
5	n-hexane	79.3	93

[a]Reaction conditions: CPE (1 mmol), TBHP (3 mmol), catalyst (0.2 mol%), solvent (1 mL), T = 60 °C, and t = 8 h. [b]GC conversion and selectivity for target product benzophenone were based on naphthalene as internal standard. All of the products were identified by GC-MS spectra and GC spectra.

Table S5. Exploration of reaction mechanism[a].

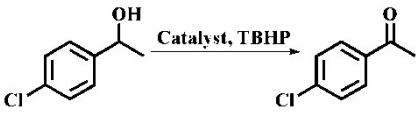

Entry	Cat.	Gas atmosphere	Conv. [b] / %
1	**CuW-TRZ** [c]	Air	36
2	**CuW-TRZ**	O_2	91
3	**CuW-TRZ**	Air	93
4	**CuW-TRZ**	N_2	90

[a] Reaction conditions: CPE (1 mmol), TBHP (3 mmol), catalyst (0.2 mol%), CH_3CN (1ml), T = 60 °C, t = 8 h. [b] GC yields for target product acetophenone was based on methylbenzene as internal standard. All of the products were identified by GC–MS spectra and GC spectra. [c] With BHT (1.2 eq.)

Table S6. Crystal data and structure refinement for **CuW-TRZ**.

Compound	**CuW-TRZ**.
Empirical formula	$C_{14}H_{14}ClCu_7GeN_{21}O_{45}W_{12}$
Formula weight	3955.48
Temperature/K	149.97
Crystal system	monoclinic
Space group	$P2_1/n$
a/Å	13.922(3)
b/Å	24.751(5)
c/Å	19.487(4)
α/°	90
β/°	96.915(6)
γ/°	90
Volume/Å^3	6666(2)
Z	4
ρ_{calc}g/cm^3	3.941
μ/mm^{-1}	23.376
F(000)	6980.0
Crystal size/mm^3	0.24 × 0.2 × 0.04
Radiation	MoKα (λ = 0.71073)
2θ range for data collection/°	4.418 to 50.2
Index ranges	-16 ≤ h ≤ 16, -29 ≤ k ≤ 29, -23 ≤ l ≤ 23
Reflections collected	54797
Independent reflections	11845 [R_{int}= 0.0633, R_σ= 0.0540]
Data/restraints /parameters	11845/42/868
Goodness-of-fit on F^2	1.035
R_1[a], wR_2[b] [I>=2σ (I)]	R_1= 0.0338, wR_2= 0.0760
R_1[a], wR_2[b] [all data]	R_1= 0.0459, wR_2= 0.0815

[a] $R_1 = \sum||Fo| - |Fc||/\sum|Fo|$; [b] $wR_2 = [\sum w(Fo^2 - Fc^2)^2/\sum w(Fo^2)^2]^{1/2}$; $w = 1/[\sigma^2(Fo^2) + (xP)^2 + yP]$, $P= (Fo^2 + 2Fc^2)/3$, where x = 0.0396, y = 112.8222 for **Cu-W-TRZ**.

Section 5 References Section

References

(1) Nobuyuki, H.; Yoshihiro, O.; Toshiyuki, I.; Yoshihisa, M. Stabilization of Tetravalent Cerium upon Coordination of Unsaturated Heteropoly tungstate Anions. *Inorg. Chem*. **1994**, *33*, 1015–1020.

(2) Dolomanov, O. V.; Bourhis, L. J.; Gildea, R. J.; Howard, J. A. K.; Puschmann, H. Olex2: A Complete Structure Solution, Refinement and Analysis Program. *J. Appl. Crystallogr*. **2009**, *42*, 339–341.

(3) Bourhis, L. J.; Dolomanov, O. V.; Gildea, R. J.; Howard, J. A. K.; Puschmann, H. The anatomy of a comprehensive constrained, restrained refinement program for the modern computing environment Olex2 dissected. *Acta Crystallogr. Sect. A Found. Adv*. **2015**, *71*, 59–76.

(4) Lu, X.; Luo, Y.; Liu, Y.; Ma, W.; Xu, Y.; Zhang, H. Assembly of Three Stable POM-Based Pillar-Layer Cu^{I} Coordination Polymers with Visible Light Driven Photocatalytic Properties. *CrystEngComm*. **2016**, *18*, 3650–3654.